arXiv:2505.11567v1 [cs.LG] 16 May 2025

Beyond Time: Cross-Dimensional Frequency Supervision for Time Series Forecasting

Tianyi Shi[1,†], Zhu Meng[1,†], Yue Chen[1], Siyang Zheng[1], Fei Su[1,2], Jin Huang[3], Changrui Ren[3], Zhicheng Zhao[1,2,*]
[1] Beijing University of Posts and Telecommunications
[2] Beijing Key Laboratory of Network System and Network Culture
[3] Beijing Academy of Blockchain and Edge Computing
[†] Equal Contribution
[*] Corresponding Author
{sty0622, bamboo, chenyue, zhengsiyang, sufei, zhaozc}@bupt.edu.cn,
{huangjin, rencr}@baec.org.cn

Abstract

Time series forecasting plays a crucial role in various fields, and the methods based on frequency domain analysis have become an important branch. However, most existing studies focus on the design of elaborate model architectures and are often tailored for limited datasets, still lacking universality. Besides, the assumption of independent and identically distributed (IID) data also contradicts the strong correlation of the time domain labels. To address these issues, abandoning time domain supervision, we propose a purely frequency domain supervision approach named cross-dimensional frequency (X-Freq) loss. Specifically, based on a statistical phenomenon, we first prove that the information entropy of the time series is higher than its spectral entropy, which implies higher certainty in frequency domain and thus can provide better supervision. Secondly, the Fourier Transform and the Wavelet Transform are applied to the time dimension and the channel dimension of the time series respectively, to capture the long-term and short-term frequency variations as well as the spatial configuration features. Thirdly, the loss between predictions and targets is uniformly computed in the frequency domain. Moreover, we plug-and-play incorporate X-Freq into multiple advanced forecasting models and compare on 14 real-world datasets. The experimental results demonstrate that, without making any modification to the original architectures or hyperparameters, X-Freq can improve the forecasting performance by an average of 3.3% on long-term forecasting datasets and 27.7% on short-term ones, showcasing superior generality and practicality. The code will be released publicly.

1 Introduction

Time series forecasting is a yet important fundamental technique with broad applications in energy management, financial trading, transportation optimization, weather prediction and healthcare monitoring. As the volume of temporal data continues to grow rapidly, enhancing forecasting accuracy has become an urgent need, and most methods have adopted the strategy of time domain supervision, which forces models to minimize point-wise errors, while the frequency domain characteristics of time series are ignored.

Recently, some studies[1, 2, 3, 4, 5, 6, 7] have found that frequency domain analysis shows distinct advantages in capturing cyclical patterns and multi-scale dependencies, which are often difficult to discern in time domain representations. They mainly focus on architectural innovations for frequency-aware modeling, such as Fourier-enhanced neural networks[5, 6, 1], Wavelet-based decomposition

Preprint. Under review.

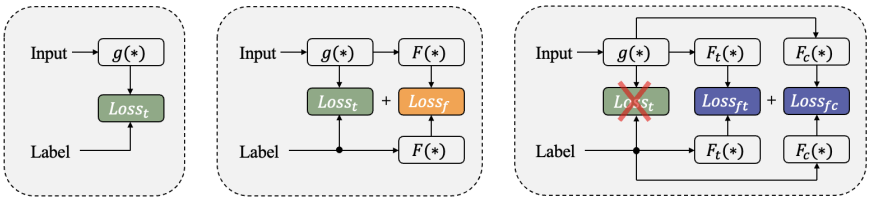

(a) Time domain supervision

(b) Time and frequency domain supervision

(c) Our frequency domain supervision

Figure 1: Three different supervision paradigms for time series forecasting.

modules[7, 8, 9], and hybrid time-frequency architectures[10]. Their supervision methods can be illustrated in Figure1 (a), which represents the classical **model-centric** time domain supervision paradigm, where the input time series are passed through a forecasting model $g(*)$ and directly aligns with the label using time domain loss such as mean squared error (MSE). These approaches typically integrate spectral operations into specific model components to enhance temporal representation learning, but still fundamentally depend on time domain alignment. Additionally, research[11, 12, 13] has shown that the strong temporal correlation in the target sequence can negatively affect forecasting models based on direct forecasting (DF).

Consequently, Wang et al.[14] attempt to incorporate frequency domain supervision losses alongside traditional time domain losses, achieving promising results in certain settings. As shown in Figure1 (b), it combines time and frequency domain information, which applies a Fourier transform, denoted as $F(*)$, along the temporal axis to both prediction and label, and computes their discrepancy $Loss_f$ to achieve frequency domain alignment. However, this approach does not fully abandon time domain losses, and the frequency domain representation remains underexplored, leading to limited generalization ability.

Despite their demonstrated effectiveness, both model-centric approaches and time-frequency hybrid supervision suffer from notable limitations. Specifically, the former has two drawbacks: (1) Their effectiveness is inherently constrained by specific architectural designs, limiting the generalizability. (2) The tight coupling between spectral operations and model structures requires complex parameter tuning, hindering practical deployment. For time-frequency hybrid supervision, two fundamental limitations persist: (1) The hybrid approaches retain time domain losses, failing to fully exploit the spectral structure of time series. (2) The higher certainty of frequency representations (due to lower spectral entropy compared to time domain entropy) suggests that purely frequency supervision can provide more stable optimization, yet this opportunity has been overlooked.

The above observations raise a crucial question: How to develop a purely frequency domain supervision approach that enables forecasting models to reduce prediction errors without any modifications to their architecture or parameters.

To address this issue, X-Freq, a purely frequency domain supervision method is proposed. Unlike previous approaches, we completely discard conventional time domain losses, and instead supervise forecasting models only in the frequency domain. Moreover, X-Freq fully exploits the frequency domain characteristics of time series along both the temporal and channel dimensions, and universally enhances various architectures without requiring any structural modifications or hyperparameter tuning.

Specifically, Figure1 (c) depicts our purely frequency domain supervision paradigm. It applies frequency transforms along both the temporal dimension F_t and the channel dimension F_c to the prediction and label sequences, and then computes frequency alignment losses along both dimensions, namely, $Loss_{ft}$ for the temporal axis and $Loss_{fc}$ for the channel axis. Experiments in Section 4 demonstrate that our supervision paradigm achieves the best generalization performance on 14 real-world datasets for both long-term and short-term forecasting.

The contributions of this paper are summarized as follows:

- We demonstrate the feasibility of completely discarding traditional time domain supervision methods and relying solely on full frequency domain supervision for time series forecasting

task. Extensive experiments show that frequency domain supervision not only remains effective but also yields better forecasting performance, offering a new perspective for leveraging frequency analysis in time series prediction.

- X-Freq, a novel model-agnostic frequency domain supervision method is proposed, which applies spectral transform along both the temporal and channel dimensions. X-Freq can be seamlessly integrated into a wide range of time series forecasting models in a plug-and-play manner, and consistently enhances their predictive performance.
- Comprehensive experiments are conducted on 14 real-world datasets across various state-of-the-art (SOTA) forecasting models. The results demonstrate that X-Freq achieves an average performance improvement of 3.3% for long-term forecasting and 27.7% for short-term forecasting, without any modification to the original model architectures, validating its effectiveness and strong generality.

2 Related Work

Time domain approaches. Traditional time series forecasting methods initially rely on classical statistical models such as ARIMA[15] and Vector AutoRegression (VAR)[16]. With the rise of neural networks, time series modeling has significantly evolved, particularly with the advent of RNN-based methods (e.g., DeepAR[17], LSTNet[18], DA-RNN[19]) and CNN-based approaches (e.g., TCN[20], SCINet[21], TimesNet[22]). The introduction of the Transformer[23] architecture, known for its exceptional modeling capacity, has led to a surge in Transformer-based forecasting models. Early examples include Informer[24], which applies Transformers directly to time series forecasting; PatchTST[25], which treats time series segments as tokens; and iTransformer[26], which integrates both temporal and channel-wise dependencies. Interestingly, DLinear[27] demonstrates the surprising effectiveness of simple linear layers in time series forecasting, prompting the development of MLP-based time domain models such as TimeXer[28] and TimeMixer[29].

Frequency domain approaches. Autoformer[5] pioneers the integration of Fourier transforms within Transformer blocks, establishing a foundation for frequency-aware time series modeling. Building on this, FEDformer[6] further proposes a frequency enhancement module, based on the principle that a sparse frequency spectrum reduces prediction error. More recently, FreTS[30] utilizes MLPs to directly learn the real and imaginary parts of sequence spectra, addressing the traditional limitations of pointwise mapping in MLPs. Similarly, WPMixer[7] applies Wavelet Transforms to the input, enabling modeling directly in the Wavelet domain. These methods leverage specialized frequency domain modules or architectures to exploit frequency-based representations, but often lack generality across models. A recent method, FreDF[14], incorporates Fourier Transform along the temporal axis directly into the MSE loss function, leading to improved performance in certain models. This approach highlights the bias introduced by temporal label autocorrelation, although it retains conventional MSE supervision in the time domain.

In contrast, we propose the X-Freq, a fully frequency domain supervision method that completely eliminates time domain losses.

3 Methodology

3.1 Motivations

Time series forecasting methods are typically divided into two categories: autoregressive[31, 32, 33] and DF[7, 26, 28]. Although autoregressive models are more intuitive, they suffer from prediction error accumulation. To avoid this, most recent approaches adopt DF, which implicitly assumes the prediction targets are IID. However, studies[11, 12, 13, 14] have shown that label sequences in most real-world datasets exhibit strong temporal correlation, which deviates significantly from the IID assumption. In contrast, such correlations tend to be much weaker in the frequency domain. Based on this insight, traditional time domain losses are abandoned in favor of a purely frequency domain supervision framework in this paper, aiming at improving predictive performance. Moreover, Parseval's theorem below reveals the equivalence between the time and frequency domains from the perspective of signal energy.

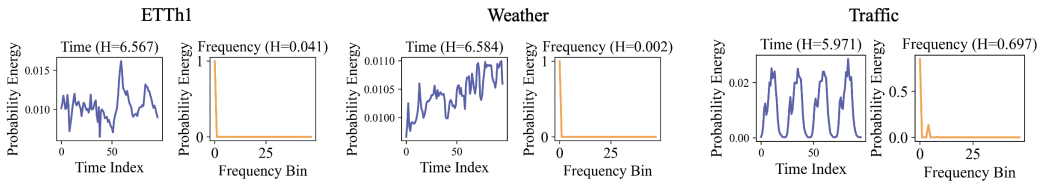

Figure 2: Visualization of the normalized time domain energy distribution and frequency domain energy spectra (for the even symmetry of the energy spectra for real-valued signals, only the positive frequency components are presented) on different datasets. H is entropy.

Specifically, let $x(t)$ be the time domain signal of interest. The total energy of the signal in the time domain is equal to that in the frequency domain. Mathematically, this relationship is expressed as

$$\int_{-\infty}^{\infty} |x(t)|^2 \, dt = \int_{-\infty}^{\infty} |X(f)|^2 \, df \tag{1}$$

where $X(f)$ is the Fourier Transform[34] of $x(t)$. The Fourier Transform is defined as $X(f) = F_f(x(t)) = \int_{-\infty}^{\infty} x(t)\, e^{-2\pi i f t} \, dt$, where i is the imaginary unit. This indicates that the frequency domain representation of a signal preserves its total energy and only redistributes it across frequency components. Therefore, applying supervision in the frequency domain does not result in any energy loss, and retains the full informational content of the original signal.

3.2 Theoretical Foundations

Recent studies[6, 35, 36] have shown that spectral entropy, which measures the complexity or unpredictability of a signal in the frequency domain, plays an important role in time series analysis. Specifically, lower spectral entropy is often associated with signals that are easier to model and predict. For example, [5, 6, 37] have leveraged frequency domain sparsity to enhance long-term forecasting accuracy, implicitly benefiting from lower spectral entropy in the frequency representation.

Building upon this insight, a theoretical justification is proposed for the use of frequency domain supervision. As formally stated in Theorem 3.2.1, the spectral energy of real-world time series datasets is more concentrated in the low-frequency range, leading to significantly lower spectral entropy in the frequency domain compared to the time domain. This entropy gap implies that frequency domain supervision provides a more compact and efficient learning signal, potentially improving model generalization and convergence.

Theorem 3.2.1 For a real-valued time series segment, if its frequency domain energy is concentrated on a few low-frequency components, then the spectral entropy in the frequency domain will be lower than that in the time domain after probability normalization.

Proof of Theorem 3.2.1 Let $x(t) \in \mathbb{R}^T$ be a univariate time series, where T is the length. Its normalized energy distribution in the time domain is $p_t(t) = |x(t)|^2 / \sum_{i=1}^{T} |x(i)|^2$, and the corresponding entropy is

$$H_t = -\sum_{t} p_t(t) \log p_t(t). \tag{2}$$

Now consider its Fourier Transform $X(f) = F_f(x(t))$, with frequency domain energy $p_f(f) = |X(f)|^2 / \sum_{i=1}^{T} |X(i)|^2$. A fixed-length Fourier Transform is applied so that $X(f)$ retains the original sequence length T, ensuring consistency across samples, and the entropy is:

$$H_f = -\sum_{f} p_f(f) \log p_f(f) \tag{3}$$

For typical time series with periodicity or strong low-frequency components, $p_f(f)$ is sharply peaked while $p_t(t)$ is often flatter. According to the principle of maximum entropy[38], $H_f < H_t$.

To validate the above theory, we visualize the energy plot and spectra of selected segments from ETTh1, Weather and Traffic datasets as probability distributions. As shown in Figure 2, the spectrum

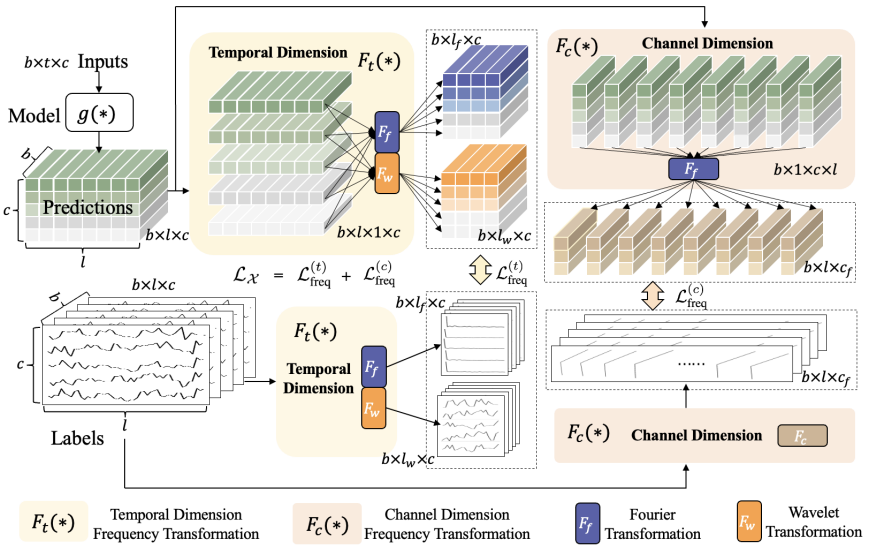

Figure 3: Supervision paradigm of X-Freq which applies frequency domain transform to align the prediction and label sequences along the temporal and channel dimensions. Specifically, $\mathcal{L}^{(t)}_{\text{freq}}$ is computed by aligning the Fourier and Wavelet Transform of predictions and labels using first-order (L1) norm along the temporal dimension. While $\mathcal{L}^{(c)}_{\text{freq}}$ is computed by aligning the Fourier Transform of the predictions and labels using the L1 norm along the channel dimension. The total loss of X-Freq is $\mathcal{L}_{\mathcal{X}} = \mathcal{L}^{(t)}_{\text{freq}} + \mathcal{L}^{(c)}_{\text{freq}}$.

of sequential signals is highly concentrated in the low-frequency region. Therefore, signals typically exhibit lower entropy in the frequency domain. These observations provide empirical support for Theory 3.2.1. Additionally, the uncertainty principle [39, 40] offers a theoretical basis for the effectiveness of frequency-based supervision. Fourier and Wavelet Transforms naturally concentrate signal energy, yielding more compact and noise-resilient representations. For instance, Wavelet decomposition suppresses noisy high-frequency components such as the HH sub-band. This energy concentration leads to a reduction in information uncertainty, which is reflected as a decrease in entropy compared to time domain representations.

3.3 X-Freq

The supervision paradigm of X-Freq is illustrated in Figure 3, where the predicted and target values are aligned entirely in the frequency domain. Specifically, suppose the shape of the input sequence for the time series forecasting models is $\mathbb{R}^{b\times t\times c}$, where b is the batch size during training, t is the sequence length and c is the number of channels. After processing through a machine learning model $g(\cdot)$, the predicted output is denoted as $\mathbf{X} \in \mathbb{R}^{b\times l\times c}$, where l represents the prediction length. To simplify notation, we only focus on a single batch instance. Let the input sequence be denoted as $X \in \mathbb{R}^{t\times c}$. The corresponding model prediction is denoted as $\hat{Y} \in \mathbb{R}^{l\times c}$, and the ground truth as $Y \in \mathbb{R}^{l\times c}$.

As shown in Figure 3, X-Freq consists of two components: the frequency domain loss along the temporal axis, denoted as $\mathcal{L}^{(t)}_{\text{freq}}$, and that along the channel axis, denoted as $\mathcal{L}^{(c)}_{\text{freq}}$. The temporal frequency domain loss is computed using both Fourier Transform and single-level Wavelet Transform[41]. It is worth noting that applying a full Fourier Transform to long non-stationary signal segments may lead to misleading frequency representations, as the global transform assumes signal stationarity and therefore fails to capture localized temporal variations. However, such non-stationary signals can often be approximated as locally stationary over short windows. In this context, a single-level Wavelet Transform can be viewed as a special case of the short-time Fourier Transform, providing localized frequency information while preserving temporal resolution. This makes it particularly effective for modeling long-term non-stationary patterns in time series data. The computation of $\mathcal{L}^{(t)}_{\text{freq}}$

is as follows:

$$\mathcal{L}_{\text{freq}}^{(t)} = \alpha \sum_{i=1}^{c} \left\| F_f(\hat{Y}_{:,i}) - F_f(Y_{:,i}) \right\|_1 + \beta \sum_{i=1}^{c} \left\| F_w(\hat{Y}_{:,i}) - F_w(Y_{:,i}) \right\|_1 \tag{4}$$

where $\hat{Y}_{:,i}$ and $Y_{:,i}$ are prediction and label sequence of the ith channel respectively, F_w denotes the Wavelet Transform, the hyperparameters α and β (where $0 < \alpha, \beta < 1$) are introduced to adjust the strength of alignment in the Fourier and Wavelet domains, respectively. Since the Fourier Transform of a real-valued signal is conjugate symmetric, only the positive frequency components are kept, and the resulting frequency domain length is $l_f = \lfloor \frac{l}{2} \rfloor + 1$. After one level of Wavelet Transform, an input signal of length l is decomposed into two parts, and the length of each part becomes $l_w = \frac{l}{2}$. It is worth noting that squared or higher-order norms for the error are not adopted. This is because, in most time series data, the magnitude of frequency components varies significantly across different bands in the frequency domain. In particular, low-frequency components typically dominate and exhibit much larger amplitudes than high-frequency components. To ensure stability of the loss, the L1 norm is adopted. Similarly, the channel-wise frequency domain loss $\mathcal{L}_{\text{freq}}^{(c)}$ is computed as follows:

$$\mathcal{L}_{\text{freq}}^{(c)} = \gamma \sum_{t=1}^{l} \left\| F_f(\hat{Y}_{t,:}) - F_f(Y_{t,:}) \right\|_1 \tag{5}$$

where $\hat{Y}_{t,:}$ and $Y_{t,:}$ are prediction and label sequence of the tth time step respectively, $\gamma > 0$ is the hyperparameter to adjust the strength of channel dimension loss and $\alpha + \beta + \gamma = 1$. Similar to the Fourier Transform along the temporal axis, applying the Fourier Transform to the channel features results in a transformed dimension of $c_f = \lfloor \frac{c}{2} \rfloor + 1$. Finally, the X-Freq loss $\mathcal{L}_{\mathcal{X}}$ is defined as a linear combination of the frequency domain losses along the temporal and channel dimensions:

$$\mathcal{L}_{\mathcal{X}} = \mathcal{L}_{\text{freq}}^{(t)} + \mathcal{L}_{\text{freq}}^{(c)} \tag{6}$$

By thoroughly exploiting frequency components along both temporal and channel dimensions, X-Freq provides strong adaptability across various model architectures.

4 Experiments

The performance of X-Freq is evaluated on 14 public datasets, including long-term and short-term forecasting.

Long-term forecasting. The performance of X-Freq for long-term forecasting is evaluated on 9 publicly available datasets across various domains, including ETT[26] (4 subsets), Weather[26], ILI[42], Exchange[26], Electricity (ECL)[26], and Traffic[26]. In accordance with commonly adopted protocols, each dataset is divided into training (60%), validation (20%) and test (20%) subsets. For all datasets except ILI, four forecast horizons {96,192,336,720} are used. For ILI, the prediction lengths {24,36,48,60} are adopted following prior works. The average forecasting errors are reported in Table 1. Without modifying any baseline model architecture or parameters, X-Freq improves 3.3% on average compared to the original evaluation metrics, which demonstrates the generalization of X-Freq.

Short-term forecasting. For short-term time series forecasting tasks, X-Freq is evaluated on 5 datasets, including PEMS[26] (4 subsets) and Solar[26], using iTransformer as the baseline model. The dataset split follows the same protocol as in long-term forecasting. For the Solar dataset, the standard forecasting lengths {96,192,336,720} are adopted, while {12,24,48,96} are used on other datasets. The forecasting errors are presented in Table 2. Without any modification to the baseline model architecture or hyperparameters, the evaluation metrics are improved by 27.7% on average. Notably, X-Freq achieves significant gains on the 96-step predictions for PEM03 and PEM07, demonstrating that frequency domain supervision can effectively mitigate the impact of temporal domain noise on model performance.

Large language model with X-Freq. Recently, large language model (LLM)-based approaches[43, 44, 45, 46] for time series forecasting have emerged rapidly. X-Freq is evaluated on two SOTA

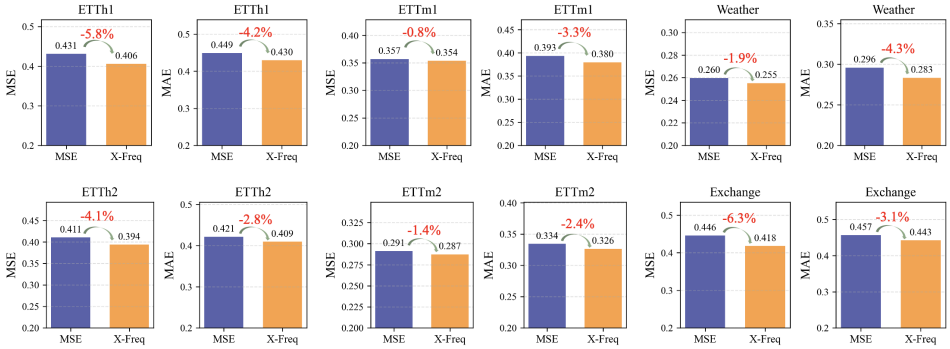

Figure 4: Comparison of forecasting errors between X-Freq and baselines on LLM-based forecasting methods. The top row shows results of the AutoTimes[33], and the bottom row for the TimeCMA[47].

Table 1: Performance of X-Freq on long-term time series datasets. Lower forecasting errors indicate better performance. The best results are highlighted in bold. TDS denotes the temporal domain supervision method corresponding to each baseline. Except for WPMixer, which uses the Smooth L1 loss, all other methods adopt the MSE loss. In the subsequent figures and tables, unless otherwise specified, TDS refers to the MSE loss in time domain.

Dataset	Loss	WPMixer (AAAI 2025) MSE	WPMixer MAE	TimeMixer (ICLR 2024) MSE	TimeMixer MAE	iTransformer (ICLR 2024) MSE	iTransformer MAE	TimeXer (NeurIPS 2024) MSE	TimeXer MAE	DLinear (AAAI 2023) MSE	DLinear MAE	Average
ETTh1	TDS	0.379	0.409	0.447	0.440	0.454	0.448	0.437	0.437	0.423	0.437	0.431
	X-Freq	**0.376**	**0.406**	**0.435**	**0.429**	**0.444**	**0.437**	**0.436**	**0.429**	**0.413**	**0.424**	**0.423**
ETTh2	TDS	0.309	0.370	0.374	0.401	0.383	0.407	0.368	0.396	0.431	0.447	0.388
	X-Freq	**0.308**	**0.368**	**0.368**	**0.394**	**0.376**	**0.400**	**0.363**	**0.389**	**0.415**	**0.434**	**0.381**
ETTm1	TDS	0.336	0.373	0.381	0.396	0.407	0.410	0.382	0.397	0.357	0.379	0.382
	X-Freq	**0.333**	**0.368**	**0.378**	**0.385**	**0.397**	**0.398**	**0.377**	**0.385**	**0.353**	**0.372**	**0.375**
ETTm2	TDS	**0.246**	0.307	0.275	0.323	0.288	0.332	0.274	0.322	0.267	0.332	0.297
	X-Freq	**0.246**	**0.303**	**0.273**	**0.319**	**0.283**	**0.324**	**0.271**	**0.315**	**0.263**	**0.322**	**0.292**
Weather	TDS	**0.217**	**0.252**	**0.240**	0.272	0.258	0.278	0.241	0.271	0.246	0.300	0.257
	X-Freq	**0.217**	**0.252**	0.242	**0.266**	**0.255**	**0.275**	**0.239**	**0.266**	**0.240**	**0.280**	**0.253**
Exchange	TDS	0.362	0.406	0.352	0.398	0.360	0.403	0.372	0.409	0.367	0.416	0.384
	X-Freq	**0.342**	**0.396**	**0.342**	**0.393**	**0.353**	**0.401**	**0.349**	**0.398**	**0.315**	**0.394**	**0.368**
ILI	TDS	1.584	0.817	2.088	0.977	2.552	1.109	2.143	0.961	2.169	1.041	1.544
	X-Freq	**1.536**	**0.783**	**1.739**	**0.828**	**2.516**	**1.097**	**2.124**	**0.944**	**2.049**	**0.970**	**1.459**
ECL	TDS	**0.158**	0.251	**0.182**	0.273	0.178	0.270	**0.171**	0.270	**0.166**	0.264	0.218
	X-Freq	**0.158**	**0.250**	0.183	**0.272**	**0.169**	**0.258**	0.172	**0.268**	0.167	**0.263**	**0.216**
Traffic	TDS	0.386	0.264	0.499	0.322	0.428	0.282	**0.466**	0.287	0.434	0.295	0.366
	X-Freq	**0.383**	**0.261**	**0.496**	**0.308**	**0.421**	**0.270**	0.468	**0.277**	**0.433**	**0.293**	**0.361**
Average	TDS	0.442	0.383	0.538	0.422	0.590	0.437	0.539	0.416	0.540	0.434	0.474
	X-Freq	**0.433**	**0.376**	**0.495**	**0.399**	**0.579**	**0.429**	**0.533**	**0.408**	**0.517**	**0.417**	**0.459**
Improvement		**2.0%**	**1.8%**	**8.0%**	**5.5%**	**1.8%**	**2.0%**	**1.1%**	**2.1%**	**4.3%**	**4.0%**	**3.3%**

LLM-based architectures: the autoregressive forecasting model AutoTimes[33] and the cross-modal prediction model TimeCMA[47]. As shown in Figure 4, the top row compares the average forecasting errors of the AutoTimes baseline and its X-Freq-enhanced variant under four prediction lengths {96,192,336,720}; the bottom row shows the results for TimeCMA. Without making any modifications to the model architectures, X-Freq achieves an average improvement of 3.4% in forecasting performance.

Ablation Study. A detailed ablation study is conducted on the Weather dataset using the SOTA WPMixer model to examine the contributions of three frequency domain loss components in X-Freq: the channel-wise frequency loss, the temporal-axis Fourier loss and Wavelet loss. As shown in Table 3, when used individually, the Wavelet-based temporal-axis loss performs the worst. This is because Wavelet Transform is essentially a form of short-time Fourier Transform, which preserves partial temporal correlations in long sequences. For direct prediction models, such residual temporal dependencies can interfere with the model's ability to learn generalizable patterns. However, when combined with the other two frequency domain losses, the Wavelet component contributes positively and helps unlock the full potential of X-Freq, leading to more accurate forecasts.

Table 2: Performance of X-Freq on short-term time series forecasting datasets. Lower values indicate better performance with iTransformer. The best results are highlighted in bold.

Dataset	Loss	12 (96)		24 (192)		48 (336)		96 (720)		Average	Improvement
		MSE	MAE	MSE	MAE	MSE	MAE	MSE	MAE		
PEMS03	TDS	0.069	0.174	0.098	0.209	0.165	0.276	1.149	0.792	0.366	**47.8%**
	X-Freq	**0.067**	**0.171**	**0.094**	**0.203**	**0.152**	**0.263**	**0.240**	**0.341**	**0.191**	
PEMS04	TDS	0.081	0.189	0.100	0.213	0.132	0.245	0.170	0.281	0.176	**5.5%**
	X-Freq	**0.077**	**0.182**	**0.096**	**0.205**	**0.123**	**0.234**	**0.153**	**0.264**	**0.167**	
PEMS07	TDS	0.066	0.164	0.087	0.189	0.351	0.427	1.038	0.859	0.398	**64.2%**
	X-Freq	**0.062**	**0.158**	**0.081**	**0.183**	**0.102**	**0.203**	**0.125**	**0.227**	**0.143**	
PEMS08	TDS	0.088	0.193	0.138	0.243	0.259	0.293	0.424	0.422	0.258	**16.1%**
	X-Freq	**0.086**	**0.190**	**0.134**	**0.238**	**0.213**	**0.260**	**0.292**	**0.315**	**0.216**	
Solar	TDS	0.203	0.237	0.233	0.261	0.248	0.273	**0.249**	0.275	0.247	**4.9%**
	X-Freq	**0.190**	**0.212**	**0.223**	**0.237**	**0.244**	**0.253**	0.257	**0.266**	**0.235**	

Table 3: Ablation study of X-Freq on channel-wise frequency transform (C), temporal Fourier Transform (L), and Wavelet Transform (W). The best results are highlighted in bold.

C	L	W	96		192		336		720		Average	
			MSE	MAE	MSE	MAE	MSE	MAE	MSE	MAE	MSE	MAE
✓	✗	✗	0.14039	0.18613	0.18593	0.23159	0.23507	0.27071	0.30730	0.32331	0.21717	0.25294
✗	✓	✗	0.14076	0.18610	0.18343	0.22882	0.23612	0.27169	0.30960	0.32697	0.21748	0.25340
✗	✗	✓	0.41796	0.29545	0.23048	0.25008	0.33001	0.31347	0.31005	**0.32189**	0.32213	0.29522
✓	✓	✗	0.13949	0.18499	0.18372	0.22883	0.23473	0.26984	0.30855	0.32511	0.21662	0.25219
✗	✓	✓	0.14129	0.18546	0.18313	0.22744	0.23550	0.26992	0.30748	0.32329	0.21685	0.25153
✓	✗	✓	0.14036	0.18545	0.18635	0.23172	0.23485	0.26998	0.30693	0.32240	0.21712	0.25239
✓	✓	✓	**0.13939**	**0.18425**	**0.18308**	**0.22777**	**0.23460**	**0.26962**	**0.30635**	0.32241	**0.21586**	**0.25101**

Comparison with Time and Frequency Hybrid Supervision. FreDF[14] is the first work to introduce frequency domain transformations into the supervision stage of time series forecasting. It demonstrated strong performance on models such as Autoformer[5] and iTransformer[26], and highlighted the inconsistency between the causal autocorrelation of labels in the time domain and DF architectures. However, FreDF still retains the traditional time domain MSE loss, and its frequency domain transformation is limited to Fourier Transform along the temporal-axis, leaving much of the frequency information space unexplored. Beyond the basic DLinear model originally used in FreDF, performance is further evaluated on more advanced architectures such as WPMixer[7] and TimeXer[28]. As shown in Table 4, X-Freq consistently delivers more generalizable and superior predictive gains.

Hyperparameter Sensitivity. We further analyze the effect of balancing X-Freq loss across the channel and temporal dimensions on forecasting performance. Figure 5 presents the prediction errors (MSE in the top row and MAE in the bottom row) of DLinear, iTransformer, and WPMixer on the Weather dataset with a forecast length of 720. In each plot, γ denotes the weight assigned to the channel-axis loss component. Overall, the three models exhibit relatively low sensitivity to the specific allocation of loss weights between the channel and temporal axes, with a maximum deviation

Table 4: Comparison of forecasting errors between X-Freq and FreDF across mainstream models. Lower values indicate better performance. The best results are highlighted in bold.

Dataset	Length	DLinear				TimeXer				WPMixer			
		FreDF		X-Freq		FreDF		X-Freq		FreDF		X-Freq	
		MSE	MAE	MSE	MAE	MSE	MAE	MSE	MAE	MSE	MAE	MSE	MAE
ETTh1	96	0.366	0.388	**0.365**	**0.386**	0.390	0.401	**0.378**	**0.391**	0.347	0.382	**0.345**	**0.379**
	192	**0.402**	0.410	**0.402**	**0.408**	0.448	0.439	**0.430**	**0.423**	0.382	0.409	**0.378**	**0.404**
	336	**0.428**	0.429	0.429	**0.428**	0.500	0.470	**0.470**	**0.442**	0.375	**0.407**	**0.379**	0.408
	720	0.455	0.477	**0.453**	**0.474**	0.532	0.516	**0.465**	**0.459**	0.412	0.441	**0.401**	**0.431**
	Average	0.413	0.426	**0.412**	**0.424**	0.468	0.456	**0.436**	**0.429**	0.379	0.410	**0.376**	**0.406**
ETTm1	96	0.299	0.342	**0.275**	**0.329**	0.361	0.387	**0.311**	**0.345**	0.276	0.334	**0.275**	**0.329**
	192	0.333	0.362	**0.304**	**0.343**	0.435	0.426	**0.357**	**0.371**	0.318	0.361	**0.311**	**0.352**
	336	0.366	0.382	**0.346**	**0.378**	0.458	0.441	**0.389**	**0.394**	**0.344**	0.381	0.346	**0.378**
	720	0.420	0.414	**0.399**	**0.413**	0.538	0.485	**0.451**	**0.431**	**0.399**	0.414	**0.399**	**0.413**
	Average	0.355	0.375	**0.333**	**0.368**	0.448	0.435	**0.377**	**0.385**	0.334	0.372	**0.333**	**0.368**
Weather	96	0.171	0.223	**0.171**	**0.217**	0.168	0.223	**0.155**	**0.198**	0.141	**0.186**	**0.14**	**0.186**
	192	0.212	0.263	**0.211**	**0.257**	0.228	0.275	**0.202**	**0.242**	**0.183**	**0.229**	0.185	0.23
	336	0.258	0.303	**0.256**	**0.296**	0.285	0.313	**0.259**	**0.285**	0.236	0.271	**0.235**	**0.271**
	720	0.322	0.357	**0.320**	**0.351**	0.365	0.364	**0.338**	**0.337**	0.308	0.325	**0.306**	**0.322**
	Average	0.241	0.286	**0.240**	**0.280**	0.261	0.294	**0.239**	**0.266**	**0.217**	0.253	**0.217**	**0.252**

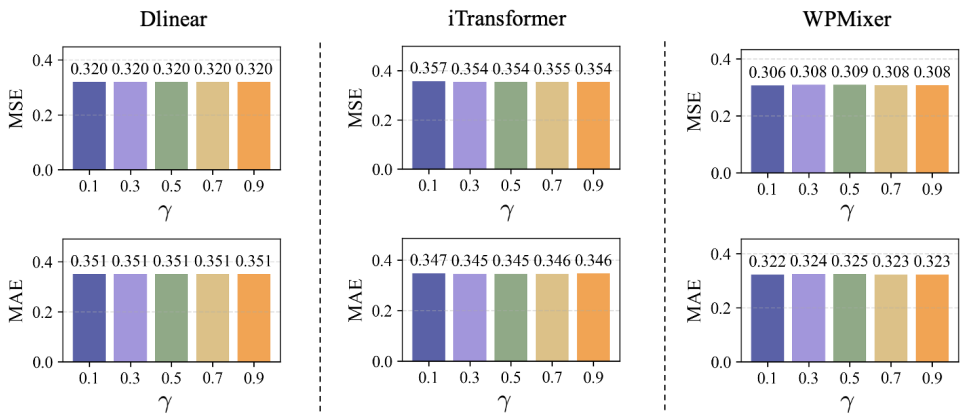

Figure 5: Impact of the ratio between channel-wise and temporal frequency losses in X-Freq on forecasting error on Weather dataset. X-Freq is insensitive to the choice of γ.

of only 0.9% across all settings. More specifically, iTransformer shows slightly better performance with larger channel-axis loss weights, due to its holistic modeling of global sequence information.

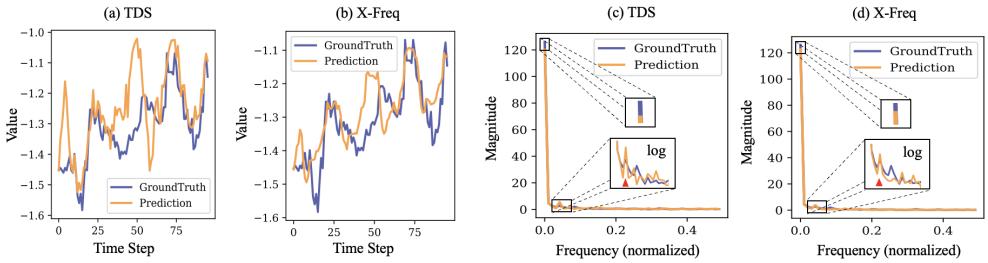

Figure 6: Time domain and frequency domain comparisons of DLinear trained with time domain supervision (a, c) and X-Freq supervision (b, d) on ETTh1. X-Freq achieves better low-frequency alignment and an improvement in time domain fidelity.

Visualization. Here, we further discuss a question: whether discarding time domain supervision will lead to overfitting to spurious frequency components and potentially distort temporal patterns. To answer this, both time and frequency domain predictions on the ETTh1 dataset are visualized. Figure 6 (a) and (c) show DLinear trained with time domain supervision (MSE), while (b) and (d) show results using X-Freq. Compared to (a), the forecast in (b) aligns more closely with the ground truth, owing to improved low-frequency modeling. This is confirmed in (d), where the lowest-frequency band is better preserved, and the secondary impulse (red triangle) is more accurately captured. Log-scaling is applied due to scale differences across components. These results indicate that frequency domain supervision not only maintains temporal fidelity but can enhance it by guiding the model toward meaningful spectral features.

5 Conclusion

In this paper, we present X-Freq, the first purely frequency domain supervision method for time series forecasting. Through spectral entropy theory and extensive experiments on 14 public datasets, we demonstrate that replacing time domain losses with cross-dimensional frequency supervision can bring about performance consistent improvements (on average 3.3% for long-term and 27.7% for short-term forecasting) without architectural modifications. Meanwhile, the plug-and-play applicability of X-Freq across diverse models also shows the great potential of frequency domain supervision, which provides a new and practical training paradigm.

References

[1] Kun Yi, Jingru Fei, Qi Zhang, Hui He, Shufeng Hao, Defu Lian, and Wei Fan. Filternet: Harnessing frequency filters for time series forecasting. *Advances in Neural Information Processing Systems*, 37:55115–55140, 2024.

[2] Xihao Piao, Zheng Chen, Taichi Murayama, Yasuko Matsubara, and Yasushi Sakurai. Fredformer: Frequency debiased transformer for time series forecasting. In *Proceedings of the 30th ACM SIGKDD Conference on Knowledge Discovery and Data Mining*, pages 2400–2410, 2024.

[3] Wei Fan, Kun Yi, Hangting Ye, Zhiyuan Ning, Qi Zhang, and Ning An. Deep frequency derivative learning for non-stationary time series forecasting. *arXiv preprint arXiv:2407.00502*, 2024.

[4] Yushu Chen, Shengzhuo Liu, Jinzhe Yang, Hao Jing, Wenlai Zhao, and Guangwen Yang. A joint time-frequency domain transformer for multivariate time series forecasting. *Neural Networks*, 176:106334, 2024.

[5] Haixu Wu, Jiehui Xu, Jianmin Wang, and Mingsheng Long. Autoformer: Decomposition transformers with auto-correlation for long-term series forecasting. *Advances in neural information processing systems*, 34:22419–22430, 2021.

[6] Tian Zhou, Ziqing Ma, Qingsong Wen, Xue Wang, Liang Sun, and Rong Jin. Fedformer: Frequency enhanced decomposed transformer for long-term series forecasting. In *International conference on machine learning*, pages 27268–27286. PMLR, 2022.

[7] Md Mahmuddun Nabi Murad, Mehmet Aktukmak, and Yasin Yilmaz. Wpmixer: Efficient multi-resolution mixing for long-term time series forecasting. In *Proceedings of the AAAI Conference on Artificial Intelligence*, volume 39, pages 19581–19588, 2025.

[8] William Gouvêa Buratto, Rafael Ninno Muniz, Ademir Nied, Carlos Frederico de Oliveira Barros, Rodolfo Cardoso, and Gabriel Villarrubia Gonzalez. Wavelet cnn-lstm time series forecasting of electricity power generation considering biomass thermal systems. *IET Generation, Transmission & Distribution*, 18(21):3437–3451, 2024.

[9] Stefano Frizzo Stefenon, Laio Oriel Seman, Evandro Cardozo da Silva, Erlon Cristian Finardi, Leandro dos Santos Coelho, and Viviana Cocco Mariani. Hypertuned wavelet convolutional neural network with long short-term memory for time series forecasting in hydroelectric power plants. *Energy*, 313:133918, 2024.

[10] Kun Yi, Qi Zhang, Wei Fan, Shoujin Wang, Pengyang Wang, Hui He, Ning An, Defu Lian, Longbing Cao, and Zhendong Niu. Frequency-domain mlps are more effective learners in time series forecasting. *Advances in Neural Information Processing Systems*, 36:76656–76679, 2023.

[11] Haoxuan Li, Kunhan Wu, Chunyuan Zheng, Yanghao Xiao, Hao Wang, Zhi Geng, Fuli Feng, Xiangnan He, and Peng Wu. Removing hidden confounding in recommendation: a unified multi-task learning approach. *Advances in Neural Information Processing Systems*, 36:54614–54626, 2023.

[12] Hao Wang, Tai-Wei Chang, Tianqiao Liu, Jianmin Huang, Zhichao Chen, Chao Yu, Ruopeng Li, and Wei Chu. Escm2: Entire space counterfactual multi-task model for post-click conversion rate estimation. In *Proceedings of the 45th International ACM SIGIR Conference on Research and Development in Information Retrieval*, pages 363–372, 2022.

[13] Hao Wang, Jiajun Fan, Zhichao Chen, Haoxuan Li, Weiming Liu, Tianqiao Liu, Quanyu Dai, Yichao Wang, Zhenhua Dong, and Ruiming Tang. Optimal transport for treatment effect estimation. *Advances in Neural Information Processing Systems*, 36:5404–5418, 2023.

[14] Hao Wang, Licheng Pan, Zhichao Chen, Degui Yang, Sen Zhang, Yifei Yang, Xinggao Liu, Haoxuan Li, and Dacheng Tao. Fredf: Learning to forecast in frequency domain. *arXiv preprint arXiv:2402.02399*, 2024.

[15] George EP Box and Gwilym M Jenkins. Some recent advances in forecasting and control. *Journal of the Royal Statistical Society. Series C (Applied Statistics)*, 17(2):91–109, 1968.

[16] George EP Box, Gwilym M Jenkins, Gregory C Reinsel, and Greta M Ljung. *Time series analysis: forecasting and control*. John Wiley & Sons, 2015.

[17] David Salinas, Valentin Flunkert, Jan Gasthaus, and Tim Januschowski. Deepar: Probabilistic forecasting with autoregressive recurrent networks. *International journal of forecasting*, 36(3):1181–1191, 2020.

[18] Lida Li, Kun Wang, Shuai Li, Xiangchu Feng, and Lei Zhang. Lst-net: Learning a convolutional neural network with a learnable sparse transform. In *European conference on computer vision*, pages 562–579. Springer, 2020.

[19] Yao Qin, Dongjin Song, Haifeng Chen, Wei Cheng, Guofei Jiang, and Garrison Cottrell. A dual-stage attention-based recurrent neural network for time series prediction. *arXiv preprint arXiv:1704.02971*, 2017.

[20] Shaojie Bai, J Zico Kolter, and Vladlen Koltun. An empirical evaluation of generic convolutional and recurrent networks for sequence modeling. *arXiv preprint arXiv:1803.01271*, 2018.

[21] Minhao Liu, Ailing Zeng, Muxi Chen, Zhijian Xu, Qiuxia Lai, Lingna Ma, and Qiang Xu. Scinet: Time series modeling and forecasting with sample convolution and interaction. *Advances in Neural Information Processing Systems*, 35:5816–5828, 2022.

[22] Haixu Wu, Tengge Hu, Yong Liu, Hang Zhou, Jianmin Wang, and Mingsheng Long. Timesnet: Temporal 2d-variation modeling for general time series analysis. *arXiv preprint arXiv:2210.02186*, 2022.

[23] Ashish Vaswani, Noam Shazeer, Niki Parmar, Jakob Uszkoreit, Llion Jones, Aidan N Gomez, Łukasz Kaiser, and Illia Polosukhin. Attention is all you need. *Advances in neural information processing systems*, 30, 2017.

[24] Haoyi Zhou, Shanghang Zhang, Jieqi Peng, Shuai Zhang, Jianxin Li, Hui Xiong, and Wancai Zhang. Informer: Beyond efficient transformer for long sequence time-series forecasting. In *Proceedings of the AAAI conference on artificial intelligence*, volume 35, pages 11106–11115, 2021.

[25] Yuqi Nie, Nam H Nguyen, Phanwadee Sinthong, and Jayant Kalagnanam. A time series is worth 64 words: Long-term forecasting with transformers. *arXiv preprint arXiv:2211.14730*, 2022.

[26] Yong Liu, Tengge Hu, Haoran Zhang, Haixu Wu, Shiyu Wang, Lintao Ma, and Mingsheng Long. itransformer: Inverted transformers are effective for time series forecasting. *arXiv preprint arXiv:2310.06625*, 2023.

[27] Ailing Zeng, Muxi Chen, Lei Zhang, and Qiang Xu. Are transformers effective for time series forecasting? In *Proceedings of the AAAI conference on artificial intelligence*, volume 37, pages 11121–11128, 2023.

[28] Yuxuan Wang, Haixu Wu, Jiaxiang Dong, Guo Qin, Haoran Zhang, Yong Liu, Yunzhong Qiu, Jianmin Wang, and Mingsheng Long. Timexer: Empowering transformers for time series forecasting with exogenous variables. *arXiv preprint arXiv:2402.19072*, 2024.

[29] Shiyu Wang, Haixu Wu, Xiaoming Shi, Tengge Hu, Huakun Luo, Lintao Ma, James Y Zhang, and Jun Zhou. Timemixer: Decomposable multiscale mixing for time series forecasting. *arXiv preprint arXiv:2405.14616*, 2024.

[30] Kun Yi, Qi Zhang, Wei Fan, Shoujin Wang, Pengyang Wang, Hui He, Ning An, Defu Lian, Longbing Cao, and Zhendong Niu. Frequency-domain mlps are more effective learners in time series forecasting. *Advances in Neural Information Processing Systems*, 36:76656–76679, 2023.

[31] Xinyu Yuan and Yan Qiao. Diffusion-ts: Interpretable diffusion for general time series generation. *arXiv preprint arXiv:2403.01742*, 2024.

[32] Kashif Rasul, Andrew Bennett, Pablo Vicente, Umang Gupta, Hena Ghonia, Anderson Schneider, and Yuriy Nevmyvaka. Vq-tr: Vector quantized attention for time series forecasting. In *The Twelfth International Conference on Learning Representations*, 2024.

[33] Yong Liu, Guo Qin, Xiangdong Huang, Jianmin Wang, and Mingsheng Long. Autotimes: Autoregressive time series forecasters via large language models. *Advances in Neural Information Processing Systems*, 37:122154–122184, 2024.

[34] Walter Rudin. *Real and complex analysis*. McGraw-Hill, Inc., 1987.

[35] Kurusetti Vinay Gupta, Jyotiranjan Beuria, and Laxmidhar Behera. Characterizing eeg signals of meditative states using persistent homology and hodge spectral entropy. *Biomedical Signal Processing and Control*, 89:105779, 2024.

[36] Ching-Hsue Cheng, Jing-Rong Chang, and Che-An Yeh. Entropy-based and trapezoid fuzzification-based fuzzy time series approaches for forecasting it project cost. *Technological Forecasting and Social Change*, 73(5):524–542, 2006.

[37] Tan Nguyen, Minh Pham, Tam Nguyen, Khai Nguyen, Stanley Osher, and Nhat Ho. Fourierformer: Transformer meets generalized fourier integral theorem. *Advances in Neural Information Processing Systems*, 35:29319–29335, 2022.

[38] Edwin T Jaynes. Information theory and statistical mechanics. *Physical review*, 106(4):620, 1957.

[39] Karlheinz Gröchenig. Uncertainty principles for time-frequency representations. *Advances in Gabor analysis*, pages 11–30, 2003.

[40] Wojbor A Woyczyński and Wojbor A Woyczyński. Uncertainty principle and wavelet transforms. *A First Course in Statistics for Signal Analysis*, pages 57–90, 2019.

[41] Ingrid Daubechies. *Ten lectures on wavelets*. SIAM, 1992.

[42] Chengsen Wang, Qi Qi, Jingyu Wang, Haifeng Sun, Zirui Zhuang, Jinming Wu, and Jianxin Liao. Rethinking the power of timestamps for robust time series forecasting: A global-local fusion perspective. *arXiv preprint arXiv:2409.18696*, 2024.

[43] Ming Jin, Shiyu Wang, Lintao Ma, Zhixuan Chu, James Y Zhang, Xiaoming Shi, Pin-Yu Chen, Yuxuan Liang, Yuan-Fang Li, Shirui Pan, et al. Time-llm: Time series forecasting by reprogramming large language models. *arXiv preprint arXiv:2310.01728*, 2023.

[44] Zijie Pan, Yushan Jiang, Sahil Garg, Anderson Schneider, Yuriy Nevmyvaka, and Dongjin Song. s^2-ip-llm: Semantic space informed prompt learning with llm for time series forecasting. In *Forty-first International Conference on Machine Learning*, 2024.

[45] Geon Lee, Wenchao Yu, Kijung Shin, Wei Cheng, and Haifeng Chen. Timecap: Learning to contextualize, augment, and predict time series events with large language model agents. In *Proceedings of the AAAI Conference on Artificial Intelligence*, volume 39, pages 18082–18090, 2025.

[46] Mingtian Tan, Mike Merrill, Vinayak Gupta, Tim Althoff, and Tom Hartvigsen. Are language models actually useful for time series forecasting? *Advances in Neural Information Processing Systems*, 37:60162–60191, 2024.

[47] Chenxi Liu, Qianxiong Xu, Hao Miao, Sun Yang, Lingzheng Zhang, Cheng Long, Ziyue Li, and Rui Zhao. Timecma: Towards llm-empowered time series forecasting via cross-modality alignment. *arXiv preprint arXiv:2406.01638*, 2024.